Biomodification of Cloisite Na$^+$ with L-Methionine Amino Acid and Preparation of Poly(vinyl alcohol)/Organoclay Nanocomposite Films

Shadpour Mallakpour,[1,2] **Mohammad Dinari**[1]

[1]*Organic Polymer Chemistry Research Laboratory, Department of Chemistry, Isfahan University of Technology, Isfahan 84156-83111, I. R. Iran*
[2]*Nanotechnology and Advanced Materials Institute, Isfahan University of Technology, Isfahan 84156-83111, I. R. Iran*

Received 7 October 2010; accepted 23 August 2011
DOI 10.1002/app.35540

ABSTRACT: Polymer/layered-silicate hybrids nanocomposites have attracted strong interest in today's materials research, as it is possible to achieve impressive enhancements of material properties compared to the pure polymers. In the present investigation, at first, Cloisite Na$^+$ was modified by protonated form of natural L-methionine amino acid via ion-exchange reaction to created chiral organonanoclay. Gallery spacing, interlamellar structure, and thermal stability of this novel chiral organonanoclay have been characterized using different techniques. Then it was used to fabrication of poly(vinyl alcohol) (PVA)/organonanoclay nanocomposite films (NCF)s with various compositions using solution casting method by ultrasound-assisted method. The films were characterized using Fourier transform infrared spectroscopy, X-ray diffraction (XRD), scanning electronic microscopy, and transmission electronic microscopy (TEM). Furthermore, thermal and optical clarity properties were investigated by thermogravimetric analysis and UV–visible transmission spectra, respectively. The TEM and XRD structure study revealed a coexistence of exfoliated and intercalated organonanoclay in the PVA matrix. The addition of organoclay into the PVA origins increases in the thermal decomposition temperatures of the NCFs. This enhancement in the thermal stability is owing to the presence of organonanoclay, which act as barriers to maximize the heat insulation and to minimize the permeability of volatile degradation products to the material. At the same time, the optical clarity of PVA/organonanoclay NCFs is not decreased in comparison with that of pure PVA. J Appl Polym Sci 124: 4322–4330, 2012

Key words: polymer nanocomposites; chiral organonanoclay; poly(vinyl alcohol); thermal properties; transmission electronic microscopy

---

INTRODUCTION

With increasing interest in the use of biodegradable and sustainable alternatives for mass applications, poly(vinyl alcohol) (PVA) provides an interesting point of comparative study on an oil-based synthetic material with the properties of a "green polymer."[1,2] It can be processed easily and has high water permeability and excellent oxygen barrier properties. PVA is the most commercially imperative water-soluble plastic in use that can be processed easily.[3] This polymer has a wide range of applications for instance protective strippable coatings, dip-coated articles, emulsion paints, fishing nets, ropes and paper, cement reinforcement, cosmetic and packaging industry, implants, artificial organs, contact lenses, drug delivery devices, binding of pigments and fibers, the manufacture of detergents and cleansing agents, adhesives, production of poly(vinyl butyral), also as a polymerization aid in emulsified polyvinyl acetate and polyvinyl chloride.[4–9] These applications all involve the use of the PVA in solution as its thermal degradation at about 150°C, limits its ability to be used in conventional thermoplastic processing equipment without modification. Owing to extensive application of PVA, many attempts have been accomplished to improve the properties of this polymer.[10] To overcome the limited biological performance and to enhance the mechanical and thermal properties of PVA, a new class of engineering-designed PVA nanocomposites has been introduced recently. Incorporation of less than 5 wt % of nanoclay in PVA matrix in the case of complete dispersion, improves its mechanical and thermal properties.[11] These polymer/clay nanocomposites have drawn much interest of researchers because of significant enhancement in mechanical properties,[12,13] thermal properties,[13,14] decreasing permeability,[12,15] influencing biodegradability of biodegradable polymers for biomedical

---

Correspondence to: S. Mallakpour (mallak@cc.iut.ac.ir).
Contract grant sponsors: Research Affairs Division Isfahan University of Technology (IUT), Iran Nanotechnology Initiative Council (INIC), National Elite Foundation (NEF) and Center of Excellency in Sensors, and Green Chemistry (IUT).

Journal of Applied Polymer Science, Vol. 124, 4322–4330 (2012)

applications,[16] etc., in comparison to polymers without nanoclay fillers. Owing to these properties, polymer/clay nanocomposites have potential applications in the automobile, aviation, geotextile, biomedical, and other polymer industries where the use of the polymers is abundant and property enhancement (mechanical, thermal, etc.) is the primary concern.[17]

Layered particles can be used as reinforcing fillers in their aggregated form, but they can be much more effective when the layers are exfoliated or intercalated. Among many types of nanoclay used to prepare polymer–clay nanocomposites, montmorillonite (MMT) attracts most attention mainly due to their natural availability. MMT has high ion exchange capacity, which allows modification of the interlayer space to achieve better compatibility with the host polymer.[18–21] Surface modifications of clay minerals have received attention because it allows the creation of new materials and new applications. Several routes can be used to modify clays and clay minerals.[22] The focus of surface modification of clays is materials science, because organoclays are vital to develop polymer nanocomposites. Modified clays are also used in other applications such as adsorbents of organic pollutants in soil, water, and air; rheological control agents; paints; cosmetics; refractory varnish; thixotropic fluids, etc.[23]

In previous research, PVA/MMT and PVA/organically modified MMT nanocomposites have been prepared and their properties were investigated by different research groups.[24–28] Strawhecker and Manias[29] also synthesized PVA nanocomposites to improve the processability and thermomechanical properties of pure PVA and PVA/MMT hybrids, with the emphasis on application-relevant, low-silicate-concentration hybrid materials. Even at low clay concentrations (<10 wt %), the thermomechanical properties could be substantially increased, whereas the gas permeability rate was reduced.

In this investigation, the ammonium salt of L-methionine (Met) amino acid as a novel chiral biosurfactant was used for organomodification of natural Cloisite Na^+ by ion exchange method in an aqueous solution. This modification increase organophilicity and dispersity of Cloisite Na^+ in polymer matrix. Additionally, because amino acids have potential of biodegradation, preparation of nanocomposites containing Cloisite Na^+/Met organoclay can enhances the biodegradability of the resulting nanocomposite. The obtained novel organoclay was used for fabrication of PVA/organoclay nanocomposite films (NCF)s by a solution casting method using ultrasonic energy. The recovered cast films were then characterized with Fourier transform infrared spectroscopy (FTIR), X-ray diffraction (XRD), UV–visible spectroscopy, thermogravimetric analysis (TGA), scanning electronic microscopy (SEM), and transmission electronic microscopy (TEM) techniques.

EXPERIMENTAL

Materials

The source clay, sodium MMT (Cloisite Na^+), was purchased from Southern Clay Products, Gonzales, TX. The cation exchange capacity (CEC) of Cloisite Na^+ is 92.6 mequiv/100 g as reported by suppliers. This compound was used without any further purification. L-Met amino acid, PVA with 99% saponification (M_W = 72,000 g mol^{-1}) and hydrochloric acid (HCl) were purchased from Merck Chemical (Germany) and was used as received.

Modification of Cloisite Na^+ with L-methionine amino acid

The organomodified nanoclay (Cloisite Na^+/Met) was prepared by a cation-exchange method, which is a displacement of the sodium cations of Cloisite Na^+ with the protonated form of the L-Met amino acid. Typically, 2 g of Cloisite Na^+ was mechanically stirred with 100 mL of deionized water at 80°C for 3 h to swell the layered silicates. The aqueous solutions of the L-Met amino acid was prepared separately by dissolving amino acid (1.5 times the CEC of clay) in distilled water at 80°C following by addition of stoichiometric amount of concentrated HCl to the solution. Then the dispersed clay solution was added to the solution of the ammonium salt of amino acid, and the mixture was stirred at 60°C for 6 h under mechanically stirred. The precipitate of modified clay was isolated by suction-filtration using whatman filter paper, placed in a 250-mL beaker again, and washed with 200 mL of hot water. This process was repeated three times to ensure the removal of excess ammonium salt of amino acid. The final product obtained by filtration was dried under vacuum at 60°C for 8 h. The dried cake was ground and screened with a 325-mesh sieve to obtain the Cloisite Na^+/Met organonanoclay.

Preparation of the PVA/Cloisite Na^+/Met NCFs

PVA/organonanoclay nanocomposites (NCs) were synthesized by a solution-intercalation method using ultrasound energy. Three different compositions of PVA/Cloisite Na^+/Met NCFs were prepared (5, 10, and 15 wt % Cloisite Na^+/Met in PVA) with the solution-intercalation film-casting technique. Before mixing with PVA solution, the organoclay was suspended in deionized water (>1 wt %) at 40°C under stirring for 3 h and sonicated using a MISONIX ultrasonic liquid processors, XL-2000 SERIES, the titanium sonic probe immersed in the solution, for 30 min at 40% power. For each composition, a 5 wt % solution of PVA in deionized water was made by constant stirring at 90°C for 30 min. Cloisite

$Na^{+/}$Met suspension was then added to PVA solution after which the mixture was stirred for 6 h at the 90°C. The resulting solution was again sonicated for 30 min to ensure uniform dispersion of Cloisite Na^+/Met. The solution was then casted on glass petridishes and allowed to dry at 40°C in an oven for 24 h, and then the fully dried films were peeled away from petridishes. The final NC films were strong and tear resistant materials that were also optically clear.

Characterization techniques

Fourier transforms infrared spectroscopy

FTIR spectra of the hybrid films were recorded with a Jasco-680 (Japan) spectrometer at a resolution of 4 cm^{-1}. Thin films of PVA and NCFs were made by evaporating solvent at 60°C and used for FTIR analysis. FTIR spectra of Cloisite Na^+ and Cloisite Na^+/Met as organic modifier were also collected by making their pellets in KBr as a medium. The pressed disk containing 1 mg of the sample and 100 mg of fine grade KBr was scanned at wavenumber range of 400–4000 cm^{-1}.

X-ray diffraction

XRD was used to characterize the layer conformation of Cloisite Na^+, Cloisite Na^+/Met, and PVA/Cloisite Na^+/Met NCFs, respectively. XRD of organoclay and NCFs were performed on dried powder and film samples, respectively. XRD patterns were recorded using Cu$K\alpha$ radiation (wavelength, λ = 0.15406 nm) on a Bruker, D8ADVANCE, (Germany) diffractometer operating at current of 100 mA and a voltage of 45 kV. The scanning rate was 0.05° min^{-1} in the angle range of $2\theta = 1.2$–10°. And Bragg's law $n\lambda = 2d \sin\theta$ was used to compute the d-spacing.

Thermogravimetric analysis

The thermal properties of Cloisite Na^+, Cloisite Na^+/Met, pure PVA, and PVA/Cloisite Na^+/Met NCFs were investigated by TGA with a STA503 WinTA instrument. In each case, the 10 mg specimens were heated from room temperature to 800°Cat a heating rate 10°C min^{-1} under nitrogen atmosphere.

Scanning electron microscopy

A scanning electron microscope (XL30, Philips) was used to observe the surface morphology of PVA/Cloisite Na^+/Met NCFs at an accelerating voltage of 5 kV.

Transmission electron microscopy

The dispersion of the nanoclays within the medium has been controlled by TEM (CM 120) at an accelerating voltage of 100 kV. For TEM, NCFs were suspended in water and a small drop of suspension was than deposited on the carbon coated copper grid. The inorganic components appear black/grey colored on the micrographs.

UV–visible spectroscopy

The samples for UV/vis measurements were prepared by cutting pieces of the cast films and were further dried at 60°C for 24 h. These films have thicknesses 0.1–0.3 mm. UV/vis transmission spectra of pure PVA and NCFs containing different amount of Cloisite Na^+/Met were obtained using a JASCO V-750 UV/Vis/NIR spectrophotometer in the spectra range from 200 to 800 nm at a wavelength scan rate of 60 nm min^{-1}.

RESULTS AND DISCUSSION

Preparation of organonanoclay and PVA/organonanoclay NCFs

PVA has a strong tendency to form hydrogen bonding within itself as well as with other species containing highly electronegative groups. In addition, organic and inorganic materials affect the rheological properties of MMT dispersions when they interact with the clay minerals. Organonanoclay has electronegative oxygen and hydroxyl groups, which can assist the adsorption of PVA onto its surface. In this study, the organonanoclay of ammonium salt of L-Met and Cloisite Na^+ was produced by an ion exchange reaction, where organic materials replace with the exchangeable cations on a Cloisite Na^+ (Scheme 1). During this reaction, the Cloisite Na^+ changes from hydrophilic to organophilic and is converted to an organonanoclay. PVA/organoclay NCFs were prepared by a solution intercalation film-casting method (Scheme 1). In this case, the different composites ware prepared with various percent of nanoclay than PVA weight.

Characterization methods

FTIR analysis

FTIR spectrum of Cloisite Na^+, organic modifier (protonated L-Met), and organonanoclay (Cloisite Na^+/Met) was collected by making their pellets in KBr as a medium with a Jasco-680 (Japan) spectrometer at a resolution of 4 cm^{-1}. Thin films of PVA and NCs were made by evaporating solvent at 60°C and used for FTIR analysis. Figure 1 shows the FTIR spectra of Cloisite Na^+, Met, and Cloisite Na^+/Met.

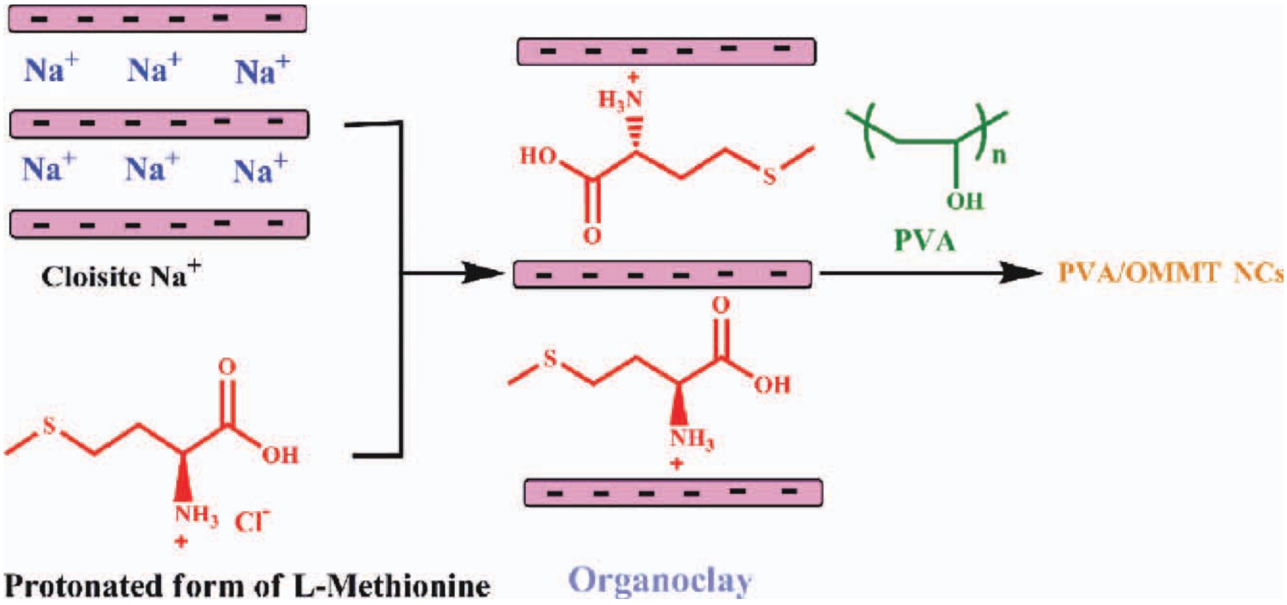

Scheme 1 Schematic illustration of the modification of Cloisite Na$^+$ with protonated L-Met and its consequent use to produce PVA/organoclay NCs. [Color figure can be viewed in the online issue, which is available at wileyonlinelibrary.com.]

In the spectrum of Cloisite Na$^+$, the absorption band at 3626 cm^{-1} is due to —OH stretching of Al—OH and Si—OH. The broad band at 3440 cm^{-1} results from the —OH stretching vibration of interlayer water. The shoulders and broadness of the structural —OH band are mainly due to contributions of several structural —OH groups occurring in the nanoclay. The characteristic peaks at 1637 and 1040 cm^{-1} is due to interlayer water deformation vibrations and Si—O stretching, respectively. The infrared spectrum of the Cloisite Na$^+$ show bands in the 400–600 cm^{-1} regions that are attributed to Si—O and Al—O bending vibration. The spectrum of bionanoclay of Cloisite Na$^+$/Met is dominated by the bands of the Cloisite Na$^+$, but the presence of the amino acid is also seen. The peaks at 1650–1400 cm^{-1} of the intercalated materials and comparison with the same wavenumber interval of the amino acid and that of the nanoclay reveal that organic cations are in the interlayer of Cloisite Na$^+$ or on its outer surface. Bands in the 3500–2500 cm^{-1} region of Met are mostly observable in the spectrum of the Cloisite Na$^+$/Met. The protonated amino acid ions should be largely among the layers since after intercalation the materials were intensively washed; thus, excess of organic cation were removed. Band at 2917 cm^{-1} is attributed to C—H stretching vibration of CH_2 aliphatic, whereas band at 1734 cm^{-1} is carbonyl group of the interlayered L-Met amino acid.

In the PVA spectrum, peaks at 2941, 1420, and 1093 cm^{-1} are attributed to the C—H stretching, C—H bending, and C—O stretching of PVA, respectively. After the addition of Cloisite Na$^+$/Met organoclay to PVA matrix, the shift of the hydroxyl peak from 3389 to 3310 cm^{-1} results from the strengthening of hydrogen bonds because of hydrogen bonding between —OH groups of PVA and silanol groups (—SiOH) of Cloisite Na$^+$. In NCF10%, the presence of the typical bands of pure PVA (3400 cm^{-1}, —OH stretching; 2900 cm^{-1}, —CH_2 stretching; 1090 cm^{-1}, C—O stretching) and Cloisite Na$^+$/Met (1050–1000 cm^{-1}, Si—O stretching; 525 and 468 cm^{-1}, Si—O—Al

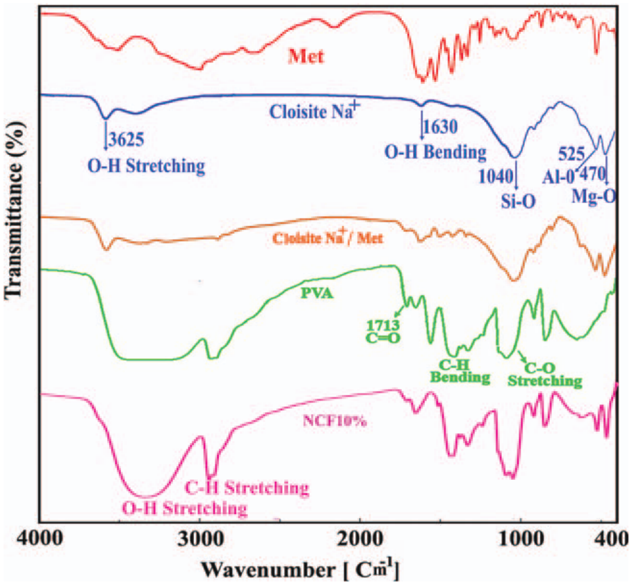

Figure 1 FTIR spectra of L-Met, Cloisite Na$^+$, Cloisite Na$^+$/Met, PVA film, and NCF10%. [Color figure can be viewed in the online issue, which is available at wileyonlinelibrary.com.]

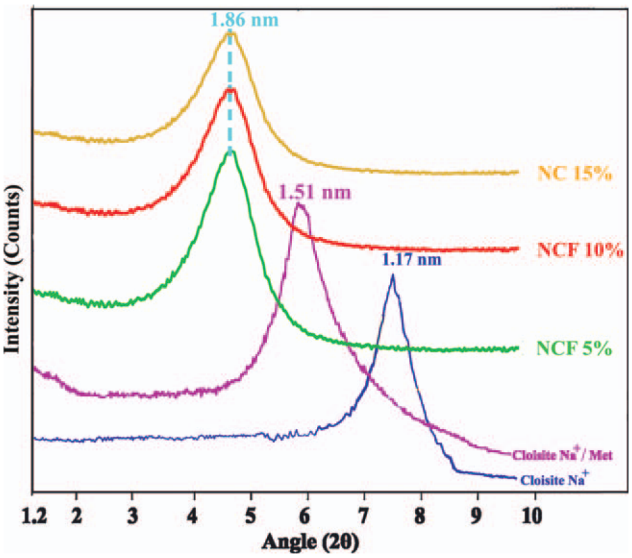

Figure 2 XRD patterns of Cloisite Na$^+$, Cloisite Na$^+$/Met, and different NCFs. [Color figure can be viewed in the online issue, which is available at wileyonlinelibrary.com.]

and Si—O—Si bending) are confirmed in the spectrum of the PVA/Cloisite Na$^+$/Met NCFs.

XRD analysis

XRD is the most useful technique to evaluate the *d*-spacing between the nanoclay layers. By monitoring the position and intensity of the basal reflections from the distributed silicate layers, the nanocomposite structure (intercalated or exfoliated) may be identified.[30] Figure 2 shows the XRD patterns of Cloisite Na$^+$, organonanoclay of Cloisite Na$^+$/Met and different NCFs (5, 10, and 15%). The theoretical basal spacing of unmodified Cloisite Na$^+$ nanoclay is 1.17 nm at $2\theta = 7.56°$. After modification of Cloisite Na$^+$ with ammonium salt of L-Met amino acid, *d*-spacing of organonanoclay has increased due to the organically modification process. An increase of the interlayer distance, leads to a shift of the diffraction peak toward lower angles. After modification, the diffraction peak for Cloisite Na$^+$/Met shifts to $2\theta = 5.84°$ and basal spacing increases from 1.17 to 1.51 nm. According to the Bragg's law, the *d*-spacing of Cloisite Na$^+$ shows an increase after modification, which indicates that Met cation has been effectively intercalated into the interlayer of Cloisite Na$^+$ and this greater *d*-spacing of organonanoclay help for the intercalation of PVA into interlayers of organoclay.

In the XRD curves of PVA/Cloisite Na$^+$/Met NCFs a diffraction peak corresponding to the basal spacing was observed at $2\theta = 4.74°$, corresponding to an interlayer distance of 1.86 nm. In these NCs with various Cloisite Na$^+$/Met content, the location of the peak indicated an increase in the basal interlayer spacing over that in Cloisite Na$^+$/Met, this indicate that the organoclay was intercalated in polymer matrix. However, theoretical and experimental studies showed that linear monodisperse polymeric chains in the vicinity of flat surfaces tend to orient with their long axes parallel to the surfaces to minimize conformational distortions to the chains. The height of such an arrangement can be quantified in 4 and 7 Å. In this study, the increase in *d*-spacing is, therefore, very small to be ascribed to the insertion of a polymeric chain. It can be concluded that the reorganization of the interlayer space or of an alteration of the organomodificant occurred due to the polymer-filler interactions. XRD results are summarized in Table I.

TABLE I
XRD data of Cloisite Na$^+$, Cloisite Na$^+$/Met, and NCF5%

Samples	2θ	*d*-spacing (nm)
Cloisite Na$^+$	7.54	1.17
Cloisite Na$^+$/Met	5.84	1.51
NCF5%	4.74	1.86

Thermogravimetric analysis

Thermal stability plays an important role in determining both technological applications and processing conditions of polymeric nanocomposites. One method for the characterization of the organoclay is the use of TGA technique. The TGA curves for Cloisite Na$^+$ and novel organoclay are shown in Figure 3. According to this figure, decomposition of Cloisite Na$^+$ occurs in two steps: the mass loss before 100°C was attributed to the desorption of water from the interlayer space, as the maximum decomposition starts at around 600°C due to dehydroxylation of the layers and proceeds till around 700°C.[31] In comparison with Cloisite Na$^+$, organoclays have lower mass

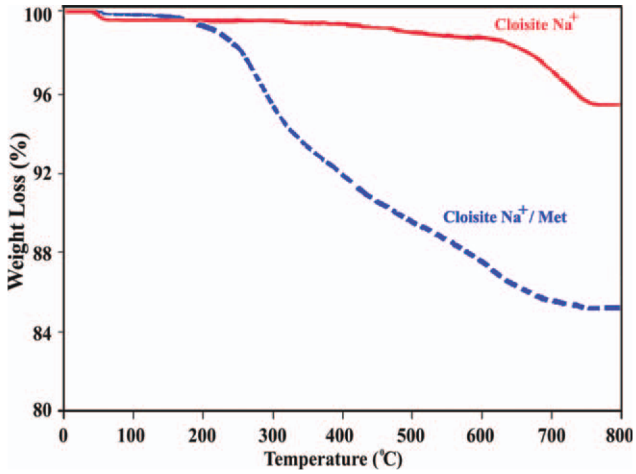

Figure 3 TGA curves for Cloisite Na$^+$ and Cloisite Na$^+$/Met. [Color figure can be viewed in the online issue, which is available at wileyonlinelibrary.com.]

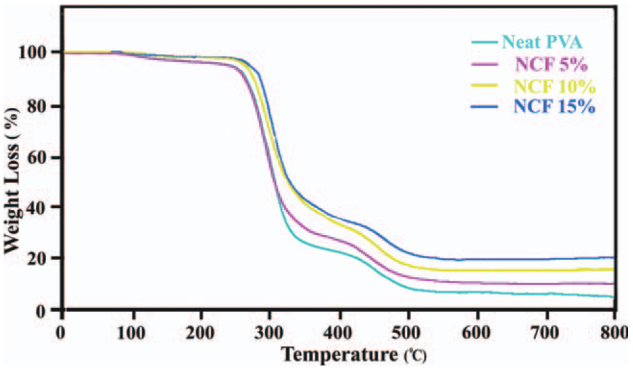

Figure 4 TGA curves of pure PVA and different NCFs. [Color figure can be viewed in the online issue, which is available at wileyonlinelibrary.com.]

loss before 100°C, implying less free water in the modified Cloisite Na^+. A possible explanation is that the presence of Cloisite Na^+/Met as a biosurfactant lowers the surface energy of the inorganic material, and converts the hydrophilic silicate surface to an organophilic one.[32] Previous studies showed that the decomposition of an organonanoclay takes place in four steps.[33,34] Moreover, there are three different molecular environments for the L-Met in the chiral organonanoclay: (1) L-Met cations intercalated into the nanoclay interlayers through cation exchange and bound to surface sites via electrostatic interaction; (2) L-Met physically adsorbed on the external surface of the clay; and (3) L-Met molecules located within the nanoclay interlayer.[33] Therefore, the decomposition temperatures for L-Met with different molecular environments will be different from each other. Cloisite Na^+ does not undergo thermally induced changes in the temperature range of 130–650°C; therefore, the mass loss in this temperature range should be attributed to the decomposition and/or evaporation of the amino acid ions. For the meantime, all different molecular environments of the amino acid ions are observed as shown in Figure 3. The peaks at 120–130, 300–330, 430–450, and 590–610°C correspond to the decomposition of the external surface, physically adsorbed L-Met, interlayer-adsorbed L-Met molecules, and intercalated L-Met cations, respectively. The results show that, at first, desorption of the physisorbed water occurred and then decarboxylation of amino acid took place. On further increase in temperature, deintercalation took place through the destruction of the organic material. At still higher temperature, the loss of structural OH groups starts until the collapse of the layered structure occurs. As shown by XRD patterns and TGA curves, the organic cations have been successfully intercalated into clay interlayers.

Thermal decomposition behavior of polymeric materials as well as polymer-based nanocomposites is usually studied by TGA technique. TGA of pure PVA and its NCFs with various Cloisite Na^+/Met percent are depicted in Figure 4, and the residual mass at different temperatures is summarized in Table II. Three weight loss stages were observed in the TGA curve for PVA film, as shown in the literature.[35] The first weight loss takes place at 50–176°C due to the evaporation of the trapped water; the second stage at 200–400°C involves the elimination reactions of water. The degradation step at 400–550°C is more complex and includes the further degradation of polyene residues to yield the carbon and hydrocarbons. The thermal decomposition of neat PVA and its Cloisite Na^+/Met NCFs are similar, as can be seen from the thermograms in Figure 4. But the NCs have higher thermal stability than that of pure PVA. According to this figure, the NCFs showed higher resistance toward thermal degradation. PVA film shows 7% residue at 800°C while the NCFs show 13–20% residue at this temperature (Table II). This improvement in the thermal stability was due to the presence of the nanolayers, which acted as barriers that maximized the heat insulation and minimized the permeability of volatile degradation products in the material. This increase was also because of the decreased permeability of oxygen, which resulted from the dispersion of organonanoclay in the polymer/organonanoclay NCFs. Based on the aforementioned results, it was concluded that the thermal stability of the hybrids was improved by the presence of the dispersed nanolayers over that of pure PVA.

Structure and morphology image studies (SEM and TEM)

The morphological image of the Cloisite Na^+, organomodified Cloisite Na^+ and NCF10% were studied by SEM. Figure 5(a–d) show the morphology of Cloisite Na^+ before and after modification. There are not many morphologic differences observed between organonanoclay despite the obvious variation observed in XRD measurements. Cloisite Na^+ shows massive, aggregated morphology and in some instances, there are some bulky flakes. Organonanoclay has more fragments of smaller size, and they are formed with irregular shapes. Conversely, the organonanoclay form

TABLE II
TGA of neat PVA and different PVA/organoclay BNC films-residual mass at different temperatures

	% Residual mass			
Temperature (°C)	Neat PVA	NC5%	NC10%	NC15%
200	97.7	98.2	98.2	98.2
300	58.6	59.1	75.6	77.3
400	22.8	27.5	35.2	37.1
500	12.7	16.3	19.4	22.7
600	8.7	13.2	17.6	21.1
700	7.1	13.0	16.8	20.2
800	7.1	13.0	16.8	20.2

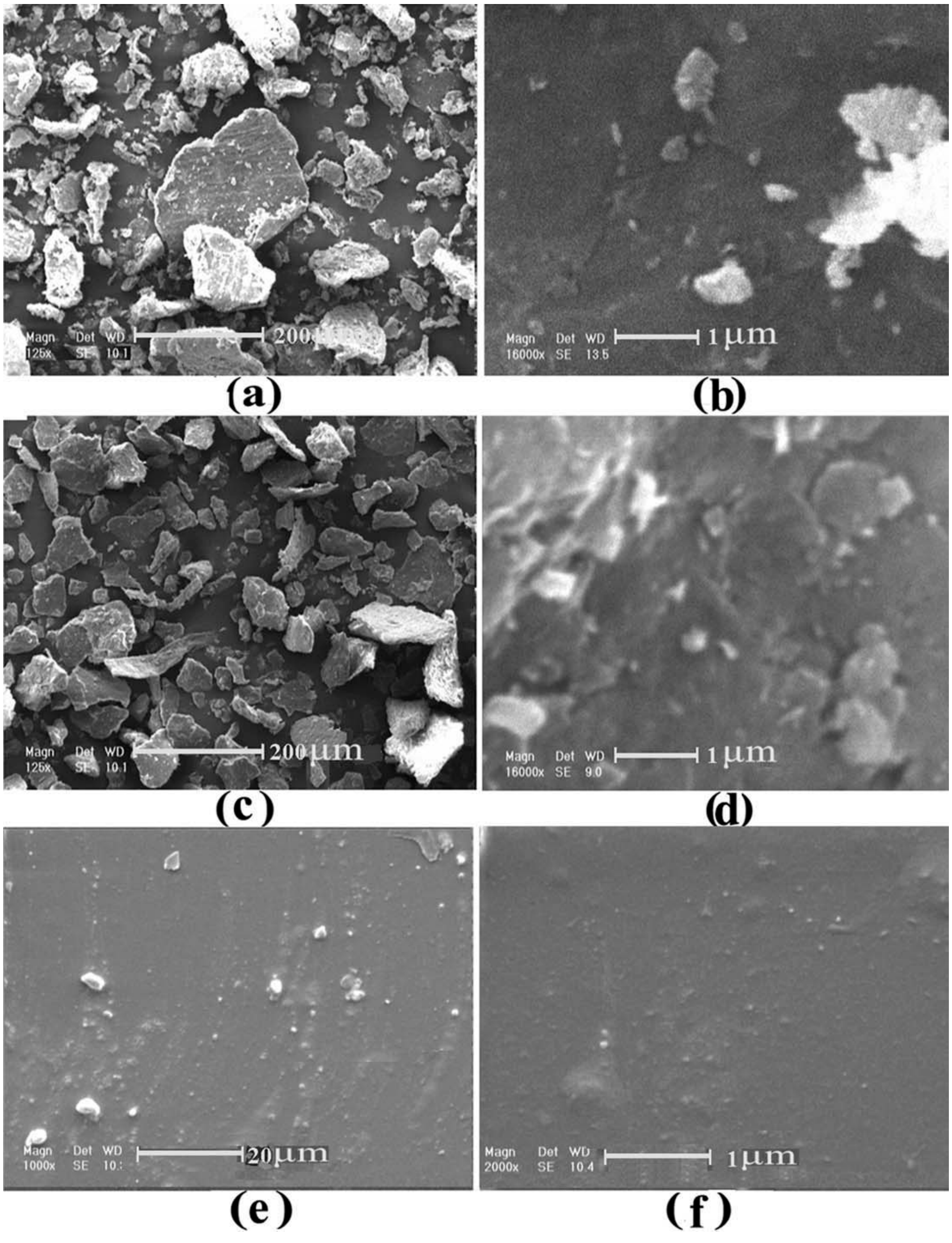

Figure 5 SEM micrographs of Cloisite Na$^+$ (a and b), Cloisite Na$^+$/Met (c and d), and NCF10% (e and f).

agglomerations and gather together much easier than those of Cloisite Na$^+$ because the surfactants compensate for the negative charge and thus eliminates the repulsive electrostatic forces between the Cloisite Na$^+$ particles. The SEM images of PVA/organonanoclay NCF10% show the flake-like structure and the high yield of organonanoclay that have the smoother morphology than organoclay [Fig. 5(e,f)].

More details about the formation of a true nanoscaled composite were provided by the TEM observation. Figure 6 shows the typical TEM image of the 10 wt % NCF in which the brighter region represents the polymer matrix while the dark narrow stripes represent the stacked and intercalated stacked nanoparticles. TEM study of the NC structure revealed a coexistence of exfoliated and intercalated Cloisite Na$^+$/Met layers. TEM observations have been complete by XRD analysis, which gives information on the interlayer distance of the aluminosilicate platelets. In Figure 6, the TEM image of NCF with 10 wt % organonanoclay loading, showed that the lamellar bionanocomposite has a mixed nanomorphology in the intercalated and the

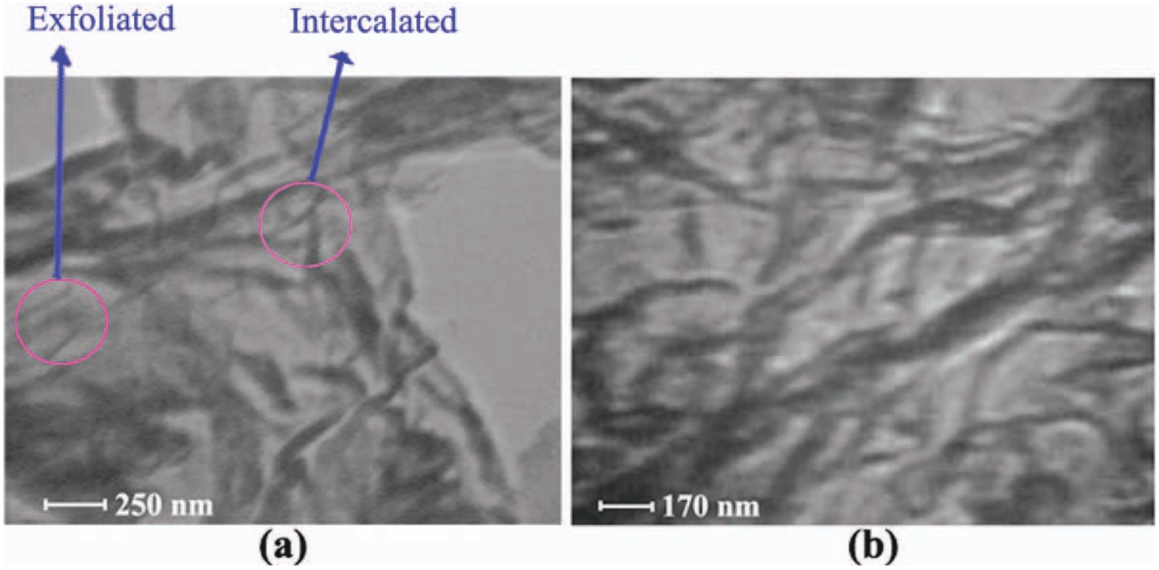

Figure 6 TEM images of PVA/Cloisite Na$^+$/Met NCF10% with different magnifications. [Color figure can be viewed in the online issue, which is available at wileyonlinelibrary.com.]

exfoliated states. The nanoclay sheets were appraised to be about 1 nm thick and an average length of about 100 nm. Intercalated layers structures talk about where the inorganic layers maintain the parallel registry of pristine silicates and are separated by ultrathin (1.3–5 mm) PVA matrix. Because of the periodic parallel assembly of the silicates, the intercalated structures give rise to XRD peaks. In addition, exfoliated layers structures mention where the layers are much further apart (5 nm), and in general, both the layer registry and the parallel stacking are lost.[36] This TEM photograph demonstrates that most of the nanoclay layers were intercalated and dispersed homogeneously into the PVA matrix.

Optical transparency of NCFs

Even though layered silicates are microns in lateral size, they are just 1 nm thick. Thus, when single layers are dispersed in a polymer matrix, the resulting nanocomposite is optically clear in visible light. Owing to the nanoscale distribution of organonanoclay in the PVA matrix, optical transparency remains high at different organonanoclay contents. This allows its possible application to paper coatings, which is one of the most common appliances for pure PVA. Figure 7 shows the UV–vis transmission spectra of pure PVA and PVA/organoclay NCs with w = 5, 10, and 15% organonanoclay content in the visible light regions (200–800 nm). The PVA and NCFs used for optical property measurements are prepared to have thickness of 0.32 mm. As shown in Figure 7, the optical clarity of PVA film is slightly affected by the presence of the low clay content. By increase the clay loading in NC films, transmission percent of the UV–visible spectra degrease. According to Figure 7, PVA/w = 5% organonanoclay NCFs show the highest transmittance among all the samples between 300 and 400 nm, which may be attributed to the homogeneous and good dispersion of organonanoclay in PVA matrix.

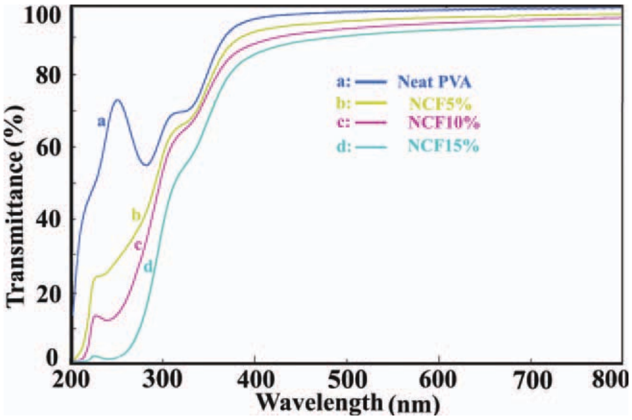

Figure 7 The effect of Cloisite Na$^+$/Met loading on optical properties of PVA/Cloisite Na$^+$ NCFs. [Color figure can be viewed in the online issue, which is available at wileyonlinelibrary.com.]

CONCLUSIONS

In this study, the structural, thermal, and optical transparency properties of PVA/Cloisite Na$^+$/Met NCs formed by film casting method in aqueous solution were studied. For this purpose, at first, Cloisite Na$^+$ was successfully modified by ammonium salt of L-Met amino acid as a novel chiral cationic surfactant. The intercalation of the Cloisite Na$^+$ by natural amino acid was confirmed by different techniques. The pristine Cloisite Na$^+$ show increased in the basal spacing after the cations exchange. Moreover, in this study, by using natural amino acid such as L-Met as a modifier for the preparation of the above organonanoclay, use of volatile and toxic common organic compound will be eliminate and provide a technology which will be environmentally benign process for the synthesis of wide variety of NC polymers. After that, a series of NCFs that consist of PVA and different concentrations of organo-modified nanoclay were synthesized by a solution-intercalation method using ultrasound energy. The obtained NCFs were investigated by FTIR spectroscopy, XRD, SEM, TEM, TGA, and UV–visible transmission spectra. TGA measurements showed that compared to the pure PVA, the addition of Cloisite Na^+/Met in the polymer matrix increase both the thermal stability and char yield. The improvement of thermal properties was attributed to the homogeneous and good dispersion of organonanoclay in polymeric matrix and the strong hydrogen bonding between O—H groups of PVA and the oxygen atoms of silicate layers or carbonyl group as well as OH group of intercalated amino acid. These changes occurred due to the fact that presence of Cloisite Na^+/Met nanolayers acts as barriers to maximize the heat insulation and to minimize the permeability of volatile degradation products to the material. Based on XRD and TEM results, a coexistence of intercalated and exfoliated Cloisite Na^+/Met exists in the final NC films. The optical clarity of PVA/organonanoclay NCs is not decreased in comparison with that of pure PVA. Some advantages of this method are (a) using natural amino acid instant of common ammonium surfactant is a safe and these natural molecule can be degradable in environment, (b) L-Met is a biodegradable molecule that causes biodegradability and biocompatibility of synthetic nanocomposites, and (c) the polar acid group (—COOH) in the amino acid can make polar interaction with OH groups of PVA chain or provide hydrogen bonding with it or with each other. These findings are important and relevant to the preparation of low-cost and potentially biodegradable chiral organonanoclay in the synthesis of novel NCs for industrial applications.

References

1. Goodship, V.; Jacobs, D. In Polyvinyl Alcohol: Materials, Processing and Applications; Ogu, E., Ed.; Rapra Review Report, Smithers Rapra Technology, United Kingdom, 2005; Vol.16, p 12.
2. Gea, S.; Bilotti, E.; Reynolds, C. T.; Soykeabkeaw, N.; Peijs, T. Mater Lett 2010, 64, 901.
3. Park, J. H.; Lee, H. W.; Chae, D. K.; Oh, W.; Yun, J. D.; Deng, Y.; Yeum, J. H. Colloid Polym Sci 2009, 287, 943.
4. Yeun, J. H.; Bang, G. S.; Park, B. J.; Ham, S. K.; Chang, J. H. J Appl Polym Sci 2006, 101, 591.
5. Chang, J. Y.; Godovsky, D. Y.; Han, M. J.; Hassan, C. M.; Kim, J.; Lee, B.; Lee, Y.; Peppas, N. A.; Quirk, R. P.; Yoo, T. Biopolymers PVA Hydrogels Anionic Polymerisation Nanocomposites; Springer: New York 2000.
6. Li, J. K.; Wang, N.; Wu, X. S. J Controlled Release 1998, 56, 117.
7. Bryaskova, R.; Pencheva, D.; Kale, G. M.; Lad, U. Kantardjie, T. J. Colloid Interface Sci 2010, 349, 77.
8. Kokabi, M.; Sirousazar, M.; Hassan, Z. M. Eur Polym J 2007, 43, 773.
9. Krumova, M.; Lopez, D.; Benavente, R.; Mijangos, C.; Perena, J. M. Polymer 2000, 41, 9265.
10. Patachia, S.; Florea, C.; Friedrich, C.; Thomann, Y. eXPRESS Polym Lett 2009, 3, 320.
11. Dayma, N.; Satapathy, B. K. Mater Des 2010, 31, 4693.
12. Pramanik, M.; Srivastava, S. K.; Biswas, K. S.; Bhowmick, A. K. J Appl Polym Sci 2003, 87, 2216.
13. Wang, D.; Wilkie, C. A. Polym Degrad Stab 2003, 80, 171.
14. Zhang, J.; Wilkie, C. A. Polym Degrad Stab 2003, 80, 163.
15. Chang, J. H.; Park, D. K. Polym Bull 2001, 47, 191.
16. Ray, S. S.; Yamada, K.; Okamoto, M.; Ueda, K. Nano Lett 2002, 2, 1093.
17. Katti, K. S.; Sikdar, D.; Katti, D. R.; Ghosh, P.; Verma, D. Polymer 2006, 47. 403.
18. Carrado, K. A. Appl Clay Sci 2000, 17, 1.
19. Patel, H. A.; Somani, R. S.; Bajaj, H. C.; Jasra, R. V. Bull Mater Sci 2006, 29, 133.
20. He, H.; Ma, Y.; Zhu, J.; Yuan, P.; Qing, Y. Appl Clay Sci 2010, 48, 67.
21. Baniasadi, H.; Ramazani, A.; Nikkhah, S. Mater Des 2010, 31, 76.
22. Bergaya, F.; Lagaly, G. Appl Clay Sci 2001, 19, 1.
23. de Paiva, L. B.; Morales, A. R.; Valenzuela Díaz, F. R. Appl Clay Sci 2008, 42, 8.
24. Chang, J. H.; Jang, T. G.; Ihn, K. J.; Lee, W. K.; Sur, G. S. J Appl Polym Sci 2003, 90, 3208.
25. Yeun, J. H.; Bang, G. S.; Park, B. J.; Ham, S. K.; Chang, J. H. J Appl Polym Sci 2006, 101, 591.
26. Nair, S. H.; Pawar, K. C.; Jog, J. P.; Badiger, M. V. J Appl Polym Sci 2007, 103, 2896.
27. Alkan, M.; Benlikaya, R. J Appl Polym Sci 2009, 112, 3764.
28. Junhao, Z.; Xiaofang, C.; He, L.; Weiliang, L. Chin J Chem 2009, 27, 1611.
29. Strawhecker, K. E.; Manias, E. Chem Mater 2000, 2, 2943.
30. Ray, S. S.; Okamoto, M. Prog Polym Sci 2003, 28, 1539.
31. Xie, W.; Gao, Z.; Pan, W. P.; Hunter, D.; Singh, A.; Vaia, R. Chem Mater 2001, 13, 2979.
32. Frost, R.; Xi, Y.; He, H. J Colloid Interface Sci 2007, 305, 150.
33. Xi, Y.; Frost, R. L.; He, H.; Kloprogge, T.; Bostrom, T. Langmuir 2005, 1, 8675.
34. Zhou, L.; Chena, H.; Jiang, X.; Lu, F.; Zhou, Y.; Yin, W.; Ji, X. J Colloid Interface Sci 2009, 332, 16.
35. Goiti, E.; Salinas, M. M.; Arias, G.; Puglia, D.; Kenny, J. M.; Mijangos, C. Polym Degrad Stab 2007, 92, 2198.
36. Strawhecker, K. E.; Manias, E. Chem Mater 2000, 12, 2943.